Optoelectronic Properties and Charge Transfer in Donor−Acceptor All-Conjugated Diblock Copolymers

Ioan Botiz,[†,⊥] Richard D. Schaller,[†,‡] Rafael Verduzco,[§] and Seth B. Darling[*,†]

[†]Center for Nanoscale Materials, Argonne National Laboratory, 9700 South Cass Avenue, Argonne, Illinois 60439, United States

[‡]Department of Chemistry, Northwestern University, 2145 Sheridan Road, Evanston, Illinois 60208, United States

[§]Department of Chemical and Biomolecular Engineering, Rice University, MS-362, 6100 Main Street, Houston, Texas 77005, United States

Ⓢ *Supporting Information*

ABSTRACT: All-conjugated block copolymers, which can self-assemble into well-ordered morphologies, provide exciting opportunities to rationally design and control the nanoscale organization of electron−donor and electron−acceptor moieties in optoelectronic active layers. Here we report on the steady-state and time-resolved optical characterization of block copolymer films and solutions containing poly-(3-hexylthiophene) as the donor block and poly(9,9-dioctylfluorene) with and without copolymerization with benzothiadiazole as the acceptor block. Transient absorption measurements suggest rapid charge transfer occurs in both systems, with higher efficiency observed in the latter composition. These results indicate that this class of materials has promise in preparing highly ordered bulk heterojunction all-polymer organic photovoltaic devices.

■ INTRODUCTION

Growing societal demand for energy is directing the attention of the scientific community toward new methodologies for converting sunlight to electricity as this resource is clean, abundant, and renewable. Decades of solar energy research are reflected by traditional photovoltaic devices that exceed power conversion efficiencies of 20% (or even 40% for multijunction cells).[1] Though such devices have tremendous value, they are currently too expensive to implement on a multi-TW scale.[2] Next-generation technologies, such as organic photovoltaics (OPVs) based on semiconducting polymeric materials, provide the prospect for implementation on a global scale due to their projected dramatic cost reductions.[3−6] One of the major impediments to achieving this potential is the rather low demonstrated power conversion efficiency of ∼8%,[7] a number well short of the thermodynamic limit.

Successful technological application of light-to-electricity conversion is associated with fundamental challenges; optimization will only be possible once these challenges are fully understood. Efficient conversion of photons to electricity in organic and hybrid materials depends on internal processes related to light absorption,[8,9] exciton separation,[10−14] and charge carrier migration,[9,15,16] among other steps. The lifetime of excitons photogenerated in organic materials translates to a maximum diffusion distance around 10 nm.[17−19] Therefore, for photovoltaic applications, the location of each exciton generated must be within ∼10 nm of a donor−acceptor (D−A) interface where the exciton can separate into a free electron and hole. Once separated, the electron and hole require continuous, and if possible straight,[20−23] pathways to the cathode and anode, respectively.

Periodic nanostructured morphologies comprised of alternating D−A domains with a characteristic distance comparable to the exciton diffusion length and perpendicularly oriented on the substrate−electrode represent the purported ideal structure within the organic or hybrid active layer. Such an ordered bulk heterojunction (BHJ) could target and optimize the above-mentioned internal processes by, for example, increasing the exciton dissociation at the D−A interfaces and diminishing nongeminate exciton recombination. Therefore, it is accepted that, in order to develop high-performance organic and/or hybrid organic−inorganic solar energy devices, it is necessary to control the active layer morphology on the nanoscale.[22,24−29]

A promising approach to generate periodic, tunable nanostructures is through the use of semiconducting D−A block copolymers (BCPs)[30,31] due to their highly tunable nanoscale self-assembly.[31−35] Besides advantages such as good solubility, lower weight, and processability on large flexible substrates, which translate to low cost,[13,27,36,37] semiconducting polymers exhibit tunable optoelectronic function,[38−42] including absorption
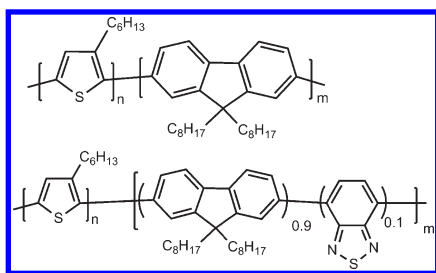
Figure 1. Schematic structure of poly(3-hexylthiophene)-*block*-poly-(9,9-dioctylfluorene) (P3HT-*b*-PFO, top) and poly(3-hexylthiophene)-*block*-poly(9,9-dioctylfluorene-*co*-benzothiadiazole) (P3HT-*b*-PFBT, bottom) diblock copolymers.

and photoluminescence,[39] bandgap,[41] enhanced carrier mobility,[42] and photovoltaic behavior.[43]

Many of the earliest conjugated BCPs relevant to optoelectronics[44,45] exhibited efficient energy transfer from donor blocks to acceptors blocks both within a single polymer chain and between neighboring chains. D−A BCPs have also been used to modestly improve photovoltaic performance by improving BHJ nanoscale structure and to target photovoltaic applications.[46−59] More examples of D−A BCPs can be found in the literature.[30,60−62] Although many of these BCPs produced ordered nanoscale morphologies, they have all displayed comparatively low power conversion efficiencies when incorporated into OPV devices. An ordered morphology providing an efficient pathway for excitons to charge separate into free charge carriers can have the unintended consequence of facilitating the recombination process across the common D−A interface. Understanding charge transfer at the D−A interface of such BCP systems remains a largely neglected area of study. The literature on BCP systems offers a limited number of experiments directly dedicated to factors that can affect charge transfer,[63,64] and generally these experiments have been limited to steady state probes.[65]

In the present work we use two newly synthesized D−A rod−rod diblock copolymers (schematically depicted in Figure 1) comprised of a poly(3-hexylthiophene) (P3HT) p-type block and a poly(9,9-dioctylfluorene) (PFO) or poly-(9,9-dioctylfluorene-*co*-benzothiadiazole) (PFBT) n-type block to study their optoelectronic and photophysical properties including charge transfer, in both solutions and thin films. While PFO has a wide bandgap and a low electron mobility not directly suitable for photovoltaic applications, its copolymerization with comonomers of benzothiadiazole[66] in PFBT lowers the bandgap and tunes the molecular orbital energy levels for more efficient charge separation. The LUMO levels of isolated P3HT and PFO are similar, suggesting only a weak tendency toward charge separation, whereas PFBT has a lower LUMO energy providing a greater driving force to accept excited electrons.[66−68] (It should be noted that molecular orbital energies of isolated molecules provide only an approximation of their properties at organic−organic heterojunctions.[69]) The random copolymer has been shown to have similar optoelectronic properties to the alternating copolymer,[66] and the 10% BT copolymer used here was selected for its solubility. We employ steady state techniques including UV−vis absorption, photoluminescence (PL) spectroscopy, and spectroelectrochemistry complemented by transient absorption (TA) spectroscopy. Our results provide insights into the optoelectronic behavior of these novel BCP systems,

including comparative analysis of subprocesses in energy conversion.

■ EXPERIMENTAL METHODS

P3HT, PFO, and PFBT homopolymers and P3HT-*b*-PFO (M_w = 16 700; PDI = 1.3) and P3HT-*b*-PFBT (M_w = 18 900; PDI = 1.4) diblock copolymers were synthesized using a combination of Grignard metathesis polymerization and Suzuki polycondensation and purified using a combination of solvent extraction and column chromatography as recently reported.[70] The P3HT-*b*-PFO and P3HT-*b*-PFBT block copolymers contained 2% and 17% P3HT homopolymer impurities, respectively. These materials were studied in both dilute solutions and thin films.

Thin solid films with thicknesses varying from 70 to 450 nm (measured by ellipsometry and atomic force microscopy) were obtained by spin-casting concentrated (10−30 mg/mL) chlorobenzene polymer solution onto clean solid substrates including boro-aluminosilicate display grade glass with and without an ITO coating. Films were solvent annealed in dichlorobenzene at 150 °C to facilitate self-assembly. ITO substrates were used as both a working electrode and substrate to deposit films for electrochemistry experiments while glass was used to prepare films suitable for UV−vis, PL, and TA studies. For the latter methods, polymer solutions of concentrations between 0.1 and 0.2 mg/mL in chloroform were also studied.

UV−vis absorption spectra were recorded using a Perkin-Elmer Lambda 950 spectrometer, and emission PL spectra were recorded using a Perkin-Elmer LS-55 luminescence spectrometer with a 250 nm/min scan rate. The excitation wavelengths were 520 and 550 nm for solutions and films, respectively.

Spectroelectrochemistry experiments were carried out using a three-electrode quartz cell consisting of an ITO-covered glass working electrode, a platinum counter electrode, and a Ag/AgCl reference electrode. The potential applied to thin polymer films deposited on the ITO working electrode was varied in steps of 0.05 V using a BASi EC Epsilon potentiostat. The supporting electrolyte was 0.1 M tetra-*n*-butylammonium hexafluorophosphate (Bu_4NPF_6) dissolved in dry acetonitrile (Fisher Scientific).

TA measurements made use of a 35 fs pulse width, 2 kHz commercial Ti:S amplifier. Tunable pulses were generated with a white-light seeded optical parametric amplifier. Time delayed pulses of white light produced in a 2 mm thick sapphire plate were used to probe the samples. Solutions were stirred, and films were constantly translated during optical measurements.

■ RESULTS AND DISCUSSION

Figure 2 shows the steady state UV−vis absorption and PL spectra for both solutions (Figure 2a,b) and films (Figure 2c,d) of P3HT, PFO, and PFBT homopolymers as well as P3HT-*b*-PFO and P3HT-*b*-PFBT diblock copolymers. To facilitate qualitative comparison, the UV−vis absorbance is normalized. P3HT homopolymer absorption is represented by a peak centered at 450 nm. PFO and PFBT homopolymers absorb maximally around 380 and 365 nm, respectively. P3HT-*b*-PFO and P3HT-*b*-PFBT diblock copolymers exhibit absorption profiles that are essentially a simple summation of those of the component blocks, with the respective contributions proportional to their stoichiometric ratio. For the BCP solutions, there is a slight red shift of the n-type block with respect to the homopolymer
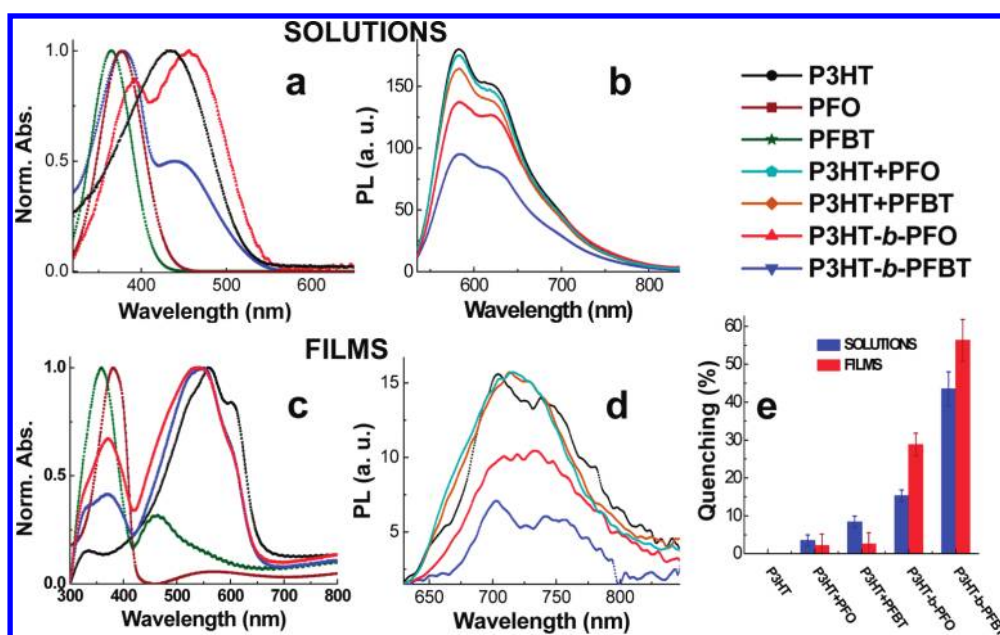
9261

dx.doi.org/10.1021/jp201344p |*J. Phys. Chem. C* 2011, 115, 9260–9266

Figure 2. Normalized UV−vis absorption spectra recorded for solutions (a) and films (c) of P3HT, PFO, PFBT, P3HT-*b*-PFO, and P3HT-*b*-PFBT along with PL spectra corresponding to solutions (b) and films (d) of P3HT, P3HT + PFO, P3HT + PFBT, P3HT-*b*-PFO, and P3HT-*b*-PFBT. PL spectra were obtained when exciting at wavelengths where only P3HT absorbs (520 nm for solutions and 550 nm for films); (e) represents a summary of quenching percentage occurring on both solutions (red) and films (blue) for materials presented in (a−d) obtained by integrating the peak area under the PL peaks.

absorption profile, likely due to subtle conformational reorganizations in the solution environment.

PFO has a wide bandgap with the lowest unoccupied molecular orbital (LUMO) level sitting only slightly below that of P3HT—at least for the separate homopolymers. Considering that the exciton binding energy associated with photoexcited P3HT is on the order of a few hundred meV, which would lower its effective LUMO even further, we do not anticipate efficient charge separation to occur at the D−A interface of P3HT-*b*-PFO. Copolymerization of substituted fluorene with comonomers of benzothiadiazole[66] leads to a PFBT product that has a lower bandgap and a concomitant lower LUMO level, which would be expected to favor electron transfer from P3HT. Thus, we anticipate a more efficient charge separation process to occur at the D−A interface of P3HT-*b*-PFBT.

A simple initial analysis of the efficiency of exciton separation in these systems is based upon steady state characterization of photoluminescence quenching. Figure 2b depicts the PL spectra recorded for different solutions (from top to bottom: P3HT, blend of P3HT and PFO homopolymers, blend of P3HT and PFBT homopolymers, P3HT-*b*-PFO, and P3HT-*b*-PFBT) each excited at 520 nm, corresponding to absorption purely in the P3HT (Figure 2a). When preparing solutions, we considered polymer molecular weights and matched the concentrations such that all solutions contained the same amount of P3HT. In these conditions, at 520 nm excitation, all solutions absorb approximately the same number of photons as confirmed by UV−vis optical density measurements. Using the area under the peak and comparing it to the area of the P3HT homopolymer peak, the degree of PL quenching can be determined. Blending P3HT homopolymer with potential electron-accepting polymers in solution leads to little or no quenching, though the P3HT/PFBT blend exhibits slightly more quenching than the P3HT/PFO blend, as anticipated based on the simple MO energy picture.

Minimal quenching is not unexpected as proximity between the disparate polymer chains is unlikely in solution, so the vast majority of the P3HT chains relax unperturbed. Covalently bonding the donor and acceptor species together in a BCP, however, has a dramatic effect on quenching due to the enforced proximity, with P3HT-*b*-PFO and P3HT-*b*-PFBT exhibiting 15% and 44% quenching, respectively. The relative effectiveness of nonradiative processes, which in this case are presumed to be charge separation events, is in agreement with the simple molecular orbital alignment picture described above. Later we provide stronger evidence, based on time-resolved measurements, to attribute the quenching to charge separation versus alternative nonradiative processes.

Additional information can be gleaned from analogous steady state experiments performed using films made of the same materials. As with the solutions, films were prepared such that the amount of P3HT contained in all films was the same. Figure 2c presents the UV−vis spectra recorded for P3HT, PFO, PFBT, P3HT-*b*-PFO, and P3HT-*b*-PFBT. In comparison to solutions, the P3HT absorption peak, in both the homopolymer and BCPs, is narrower and red-shifted by about 100 nm to a center near 550 nm, as has been reported previously in homopolymer systems.[71] Absorption peaks corresponding to PFO and PFBT are also narrowed, though the positions are similar to those observed in solutions.

Figure 2d depicts the PL spectra recorded for different films (from top to bottom: P3HT, blend of P3HT and PFO homopolymers, blend of P3HT and PFBT homopolymers, P3HT-*b*-PFO, and P3HT-*b*-PFBT) excited at 550 nm. Again, only P3HT substantially absorbs photons at this wavelength. As was observed with solutions, P3HT-*b*-PFBT exhibits the highest quenching (about 57%), suggestive of the most effective charge transfer. A substantial portion of the residual PL intensity in P3HT-*b*-PFBT solution and film samples can be attributed to the
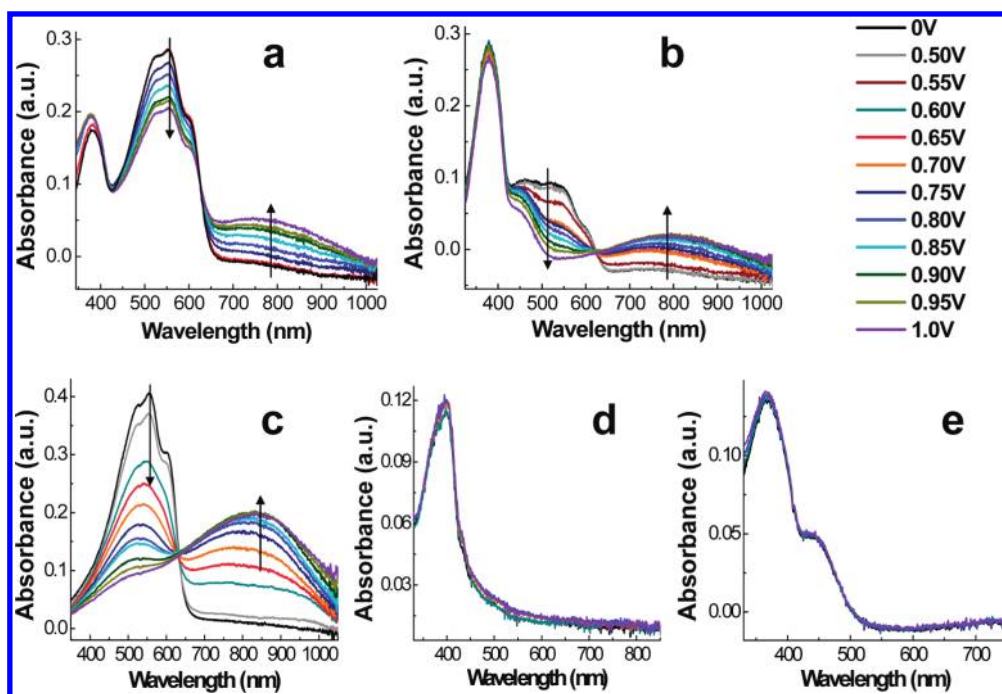
Figure 3. UV−vis−near-IR spectroelectrochemical data recorded for P3HT-*b*-PFO (a), P3HT-*b*-PFBT (b), P3HT (c), PFO (d), and PFBT (e).

Table 1. Fitting Parameters from Transient Absorption Decay Dynamics in the Near-Infrared Presented in Figure 4[a]

polymer	solutions					films				
	y_0	A_1	t_1	A_2	t_2	y_0	A_1	t_1	A_2	t_2
P3HT	0.019	0.28	160	0.48	577	0.0065	0.8	6	0.134	121
P3HT-*b*-PFO	0.028	0.32	138	0.46	630	0.017	0.83	9	0.123	146
P3HT-*b*-PFBT	0.049	0.28	106	0.53	685	0.031	0.75	24	0.176	267

[a] y_0 is the long-lived (t = infinity) baseline amplitude, and the A and t parameters are the amplitude and time constants (in picoseconds) for the two exponential decays, respectively.

P3HT homopolymer impurities. P3HT-*b*-PFO exhibits about 29% quenching, whereas in non-BCP blends of P3HT + PFO and P3HT + PFBT homopolymers the quenching is insignificant. Comparing results obtained for both solutions and films (Figure 2e), we conclude not only that P3HT-*b*-PFBT exhibits the highest quenching in both cases but also that quenching in films is more substantial, presumably due to packing of molecular chains yielding multiple acceptors in the proximity of most donors. Somewhat surprisingly, blends of P3HT + PFO and P3HT + PFBT homopolymers exhibit lower quenching in films than in solutions. This is attributed to macrophase separation that takes place when spin-casting films leading to large domains of donors and acceptors, which minimizes the D−A interfacial area in the film.

To determine an effective rate of charge separation, we first measured the excited state lifetime of P3HT in solution (see Supporting Information) to be 660 ps. Given the reported PL quantum yield (QY) of 33% for P3HT,[72] we obtained a radiative rate, k_r, of 5.0×10^8 s^{-1} as well as an intrinsic total nonradiative decay rate, k_{nr}, of 1.0×10^9 s^{-1} using QY = $k_r/(k_r + k_{nr})$. On the basis of the observed static PL quenching, we arrive at charge
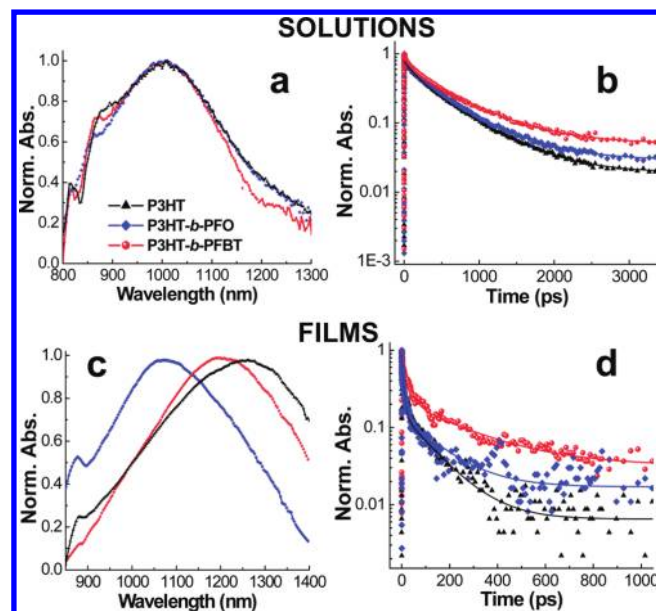

Figure 4. Near-infrared transient absorption spectra at 2 ps for solutions (a) and films (c) of P3HT, P3HT-*b*-PFO, and P3HT-*b*-PFBT and their associated dynamics at 1000 nm (b) and 1200 nm (d), respectively. In (b) and (d) the solid lines represent exponential fits through the experimental data points (fit parameters in Table 1). The pump energy was 470 nm for solutions and 550 nm for films.

transfer rates, k_{CT}, of 6.4×10^8 and 2.0×10^9 s^{-1} using QY = $k_r/(k_r + k_{nr} + k_{CT})$ and calculate charge transfer yields of 30% and 57% for solutions of P3HT-*b*-PFO and P3HT-*b*-PFBT, respectively, using $k_{CT}/(k_r + k_{nr} + k_{CT})$. The increased charge transfer yield is consistent with the expected increase in driving force upon changing from PFO to PFBT. We note that the calculated charge transfer rate of 2.0×10^9 s^{-1} for P3HT-*b*-PFBT is

competitive with intrinsic nonradiative recombination rates. Moreover, the calculated charge transfer rates represent lower limits because of the residual PL attributable to P3HT homopolymer impurities. PL quenching has, however, been shown to be a poor indicator of efficient charge photogeneration in thin films,[73] where PL quantum yield for P3HT can be below 2%.[72,74–77] Transient absorption measurements can provide details on various possible photophysical processes, including charge separation and intersystem crossing between singlet and triplet states for both polymer solutions and thin films.

Prior to delving into analysis of transient absorption results, it is informative to investigate the absorption properties of electrically charged, i.e., molecular ion, polymer species via spectroelectrochemistry. Figure 3a,b shows optical spectra of P3HT-b-PFO and P3HT-b-PFBT recorded for increasing electrode potential from 0 to 1 V. The first peak in these spectra, centered at 380 nm, corresponds to PFO or PFBT. The second absorption peak, centered at about 550 nm, is due to P3HT. P3HT-b-PFO and P3HT-b-PFBT electrochemically start to oxidize at about 0.55 V (vs Ag/AgCl). With increasing electrode potential the vibrational structure of the $\pi–\pi^*$ transition (550 nm) becomes less pronounced, which means that highly conjugated segments are oxidized first and the remaining unoxidized (uncharged) regions exhibit shorter conjugation length. In addition to bleaching of the $\pi–\pi^*$ transition, charging causes the gradual appearance of broad absorption bands in the lower energy region of the spectrum.[78] These bands are assigned to hole charge carriers on P3HT as only P3HT can be oxidized at positive potentials lower than 1 V (Figure 3c). Figure 3d,e indicates no influence of PFO and PFBT charging at these potentials. Cyclic voltammetry data (Supporting Information) indicate that in order to start oxidizing PFO and PFBT one has to apply voltages higher than 1.35 and 1.55 V, respectively.

Representative TA absorption spectra at 2 ps (Figure 4a,c) and their corresponding dynamics (Figure 4b,d) were recorded for P3HT, P3HT-b-PFO, and P3HT-b-PFBT polymer systems in solutions and thin films. TA spectra were obtained using a pump wavelength of 470 nm for solutions and 550 nm for films, respectively (Figure 4a,c). These photon energies selectively excite P3HT, though in the case of films there is a small amount of absorption in PFBT at 550 nm. Pump intensity was 75 μJ/cm^2 for all measurements. Dynamics were not significantly affected by three times higher or lower intensity. There is a consensus that the primary photoexcitations in regioregular P3HT solutions are intrachain singlet excitons[72,77] and long-lived photogenerated triplet excitons.[72,74] In thin films, the primary excitations, delocalized among neighboring lamellae layers in the film, are singlet excitons with large interchain contributions.[74,76] Direct photogeneration of charge carriers (~0.15 per absorbed photon) is also observed while long-lived photogenerated triplet excitons are not easily generated in regioregular P3HT films.[72,74,77,79] For example, transient species formed in P3HT films after excitation at 400 nm have been assigned to singlet excitons (1200 nm), polarons (1000 nm), and polaron pairs (660 nm).[79] In both films and solutions, we have recorded TA spectra at NIR wavelengths where the hole component of P3HT excitons absorb so that we can analyze their dynamics.

With this particular material system, there is not a clear spectral signature of moieties directly representing charge transfer products, so for insights into the nature of the observed steady state PL quenching we turn to the dynamics of the P3HT hole component. As seen in Figure 4b,d, the TA decay dynamics of the P3HT homopolymer differ compared to those obtained for

P3HT-b-PFO and P3HT-b-PFBT diblock copolymers (PFO and PFBT homopolymers have no TA features in the near-infrared spectral range under these conditions). The BCPs exhibit a slowed decay of the NIR induced absorption feature relative to P3HT, with P3HT-b-PFBT being even slower than P3HT-b-PFO. The P3HT dynamics are attributed to singlet exciton decay via geminate recombination (in films) or intersystem crossing to the triplet state (in solutions) as reported in the literature.[72,75,80–82] The slower BCP decay is attributed to the appearance of a population of long-lived holes residing on P3HT resulting from charge separation taking place at the D–A interface. These long-lived charges, ascribed to P3HT cations based on our spectroelectrochemistry data, contribute to the overall induced absorption in this range and therefore increase its absolute value over longer pump–probe delay times. Comparison of the BCPs and the P3HT homopolymer decays is consistent with appearance of P3HT radical cations over tens to hundreds of picoseconds, which roughly corresponds to the charge separation rates determined from the solution PL quenching data. Moreover, the amplitude of long-lived cation signal increases upon going from P3HT-b-PFO to the P3HT-b-PFBT BCP. The longer-lived P3HT holes are observed in films as well as solutions, with faster overall dynamics observed in the former, likely as a result of additional intermolecular processes. Moreover, the discrepancy in decay times between the P3HT homopolymer and the BCPs is significantly larger in films with respect to solutions. An alternative explanation for the observed slower decay in the BCP samples would be elimination of a nonradiative channel that was present in pure P3HT, but because the PL is substantially quenched in the BCPs with respect to P3HT, this mechanism is unlikely and charge separation is the most logical explanation.

CONCLUSIONS

Donor/acceptor all-conjugated block copolymers have been synthesized and characterized using a series of steady state and time-resolved optical techniques. Photoluminescence quenching in solutions and films indicates that BCPs are far more efficient at separating photogenerated excitons than blends of the same polymer block materials. Using ultrafast transient absorption spectroscopy and spectroelectrochemistry, the mechanism of the PL quenching is identified as charge transfer from P3HT to PFO or PFBT, respectively, with more efficient charge transfer in the latter. Enhanced quenching in films with respect to solutions is attributed to intermolecular processes that supplement the intramolecular charge separation observed with dilute solutions. When incorporated into photovoltaic devices, block copolymers of this nature can provide a structural platform with high nanoscale order, thereby enabling detailed structure–property studies and, ultimately, optimizing the processes underlying solar energy conversion.

ASSOCIATED CONTENT

Ⓢ Supporting Information. Cyclic voltammetry data of P3HT, PFO, and PFBT homopolymers; radiative decay of P3HT; and near-infrared transient absorption spectra of P3HT solutions and films at various delay times. This material is available free of charge via the Internet at http://pubs.acs.org.

AUTHOR INFORMATION

Corresponding Author
*E-mail: darling@anl.gov.

Present Addresses

⊥Institute of Physics, Faculty of Mathematics and Physics, Albert-Ludwig-University of Freiburg, Hermann-Herder Str. 3, 79104 Freiburg, Germany.

■ REFERENCES

(1) King, R. R.; Law, D. C.; Edmondson, K. M.; Fetzer, C. M.; Kinsey, G. S.; Yoon, H.; Sherif, R. A.; Karam, N. H. *Appl. Phys. Lett.* **2007**, *90*, 183516.

(2) Darling, S. B.; You, F.; Veselka, T.; Velosa, A. *Energy Environ. Sci.* **2011**, Advance Article.

(3) Kim, J.-Y.; Lee, K.; Coates, N. E.; Moses, D.; Nguyen, T.-Q.; Dante, M.; Heeger, A. J. *Science* **2007**, *317*, 222.

(4) Bredas, J.-L.; Durrant, J. R. *Acc. Chem. Res.* **2009**, *42*, 1689.

(5) Dennler, G.; Scharber, M. C.; Brabec, C. J. *Adv. Mater.* **2009**, *21*, 1323.

(6) Thompson, B. C.; Fréchet, J. M. J. *Angew. Chem., Int. Ed.* **2008**, *47*, 58.

(7) Solarmer Energy, Inc. Breaks Psychological Barrier with 8.13% OPV Efficiency.

(8) Dai, J.; Jiang, X.; Wang, H.; Yan, D. *Appl. Phys. Lett.* **2007**, *91*, 253503.

(9) Gadisa, A.; Mammo, W.; Andersson, L. M.; Admassie, S.; Zhang, F.; Andersson, M. R.; Inganäs, O. *Adv. Funct. Mater.* **2007**, *17*, 3836.

(10) Clarke, T. M.; Durrant, J. R. *Chem. Rev.* **2010**, *110*, 6736.

(11) Scully, S. R.; McGehee, M. D. *J. Appl. Phys.* **2006**, *100*, 034907.

(12) Lindner, S. M.; Hüttner, S.; Chiche, A.; Thelakkat, M.; Krausch, G. *Angew. Chem., Int. Ed.* **2006**, *45*, 3364.

(13) Brabec, C. J.; Sariciftci, N. S.; Hummelen, J. C. *Adv. Funct. Mater.* **2001**, *11*, 15.

(14) Salafsky, J. S.; Lubberhuizen, W. H.; Schropp, R. E. I. *Chem. Phys. Lett.* **1998**, *290*, 297.

(15) McCulloch, I.; Heeney, M.; Bailey, C.; Genevicius, K.; Macdonald I.; Shkunov, M.; Sparrowe, D.; Tierney, S.; Wagner, R.; Zhang, W. M.; Chabinyc, M. L.; Kline, R. J.; McGehee, M. D.; Toney, M. F. *Nature Mater.* **2006**, *5*, 328.

(16) Mandoc, M. M.; Kooistra, F. B.; Hummelen, J. C.; Boer, B. d.; Blom, P. W. M. *Appl. Phys. Lett.* **2007**, *91*, 263505.

(17) Yang, F.; Forrest, S. R. *ACS Nano* **2008**, *2*, 1022.

(18) Knupfer, M. *Appl. Phys. A: Mater. Sci. Process.* **2003**, *77*, 623.

(19) Stübinger, T.; Brütting, W. *J. Appl. Phys.* **2001**, *90*, 3632.

(20) Coakley, K. M.; McGehee, D. *Chem. Mater.* **2004**, *16*, 4533.

(21) Coropceanu, V.; Cornil, J.; da Silva Filho, D. A.; Olivier, Y.; Silbey, R.; Brédas, J.-L. *Chem. Rev.* **2007**, *107*, 926.

(22) Darling, S. B. *J. Phys. Chem. B* **2008**, *112*, 8891.

(23) Darling, S. B.; Sternberg, M. *J. Phys. Chem. B* **2009**, *113*, 6215.

(24) Peet, J.; Heeger, A. J.; Bazan, G. C. *Acc. Chem. Res.* **2009**, *42*, 1700.

(25) Xin, H.; Reid, O. G.; Ren, G.; Kim, F. S.; Ginger, D. S.; Jenekhe, S. A. *ACS Nano* **2010**, *4*, 1861.

(26) Yang, X.; Loos, J. *Macromolecules* **2007**, *40*, 1353.

(27) Günes, S.; Neugebauer, H.; Sariciftci, N. S. *Chem. Rev.* **2007**, *107*, 1324.

(28) van Duren, J. K. J.; Yang, X.; Loos, J.; Bulle-Lieuwma, C. W. T.; Sieval, A. B.; Hummelen, J. C.; Janssen, R. A. J. *Adv. Funct. Mater.* **2004**, *14*, 425.

(29) Sun, S.-S. *Sol. Energy Mater. Sol. Cells* **2003**, *79*, 257.

(30) Sommer, M.; Huettner, S.; Thelakkat, M. *J. Mater. Chem.* **2010**, *20*, 10788.

(31) Bates, F. S.; Fredrickson, G. H. *Phys. Today* **1999**, *52*, 32.

(32) Park, C.; Yoon, J.; Thomas, E. L. *Polymer* **2003**, *44*, 6725.

(33) Segalman, R. A. *Mater. Sci. Eng. R* **2005**, *48*, 191.

(34) Darling, S. B. *Prog. Polym. Sci.* **2007**, *32*, 1152.

(35) Ren, G.; Wu, P.-T.; Jenekhe, S. A. *ACS Nano* Articles ASAP.

(36) Forest, S. R. *Nature* **2004**, *428*, 911.

(37) Gustafsson, G.; Cao, Y.; Treacy, C. M.; Klavetter, F.; Colaneri, N.; Heeger, A. J. *Nature* **1992**, *357*, 477.

(38) Tan, Z.; Tang, R.; Zhou, E.; He, Y.; Yang, C.; Xi, F.; Li, Y. *J. Appl. Polym. Sci.* **2008**, *107*, 514.

(39) Hou, J.; Huo, L.; He, C.; Yang, C.; Li, Y. *Macromolecules* **2006**, *39*, 594.

(40) Pickup, P. G. *Mod. Aspects Electrochem.* **1999**, *33*, 549.

(41) Zhang, Q. T.; Tour, J. M. *J. Am. Chem. Soc.* **1998**, *120*, 5355.

(42) Sirringhaus, H.; Wilson, R. J.; Friend, R. H.; Inbasekaran, M.; Wu, W.; Woo, E. P.; Grell, M.; Bradley, D. D. C. *Appl. Phys. Lett.* **2000**, *77*, 406.

(43) Casalbore-Miceli, G.; Gallazzi, M. C.; Zecchin, S.; Camaioni, N.; Geri, A.; Bertarelli, C. *Adv. Funct. Mater.* **2003**, *13*, 307.

(44) Meyers, F.; Heeger, A. J.; Brédas, J. L. *J. Chem. Phys.* **1992**, *97*, 2750.

(45) Chen, X. L.; Jenekhe, S. A. *Macromolecules* **1996**, *29*, 6189.

(46) Barrau, S.; Heiser, T.; Richard, F.; Brochon, C.; Ngov, C.; van de Wetering, K.; Hadziioannou, G.; Anokhin, D. V.; Ivanov, D. A. *Macromolecules* **2008**, *41*, 2701.

(47) Stalmach, U.; de Boer, B.; Videlot, C.; van Hutten, P. F.; Hadziioannou, G. *J. Am. Chem. Soc.* **2000**, *122*, 5464.

(48) de Boer, B.; Stalmach, U.; van Hutten, P. F.; Melzer, C.; Krasnikov, V. V.; Hadziioannou, G. *Polymer* **2001**, *42*, 9097.

(49) van der Veen, M. H.; de Boer, B.; Stalmach, U.; van de Wetering, K. I.; Hadziioannou, G. *Macromolecules* **2004**, *37*, 3673.

(50) Brochon, C.; Sary, N.; Mazzenga, R.; Ngov, C.; Richard, F.; May, M.; Hadziioannou, G. *J. Appl. Polym. Sci.* **2008**, *110*, 3664.

(51) Hiorns, R. C.; Iratcabal, P.; Begue, D.; Khoukh, A.; de Bettignies R.; Leroy, J.; Firon, M.; Sentein, C.; Martinez, H.; Preud'homme, H.; Dagron-Lartigau, C. *J. Polym. Sci., Part A: Polym. Chem.* **2009**, *47*, 2304.

(52) Heiser, T.; Adamopoulos, G.; Brinkmann, M.; Giovanella, U.; Ould-Saad, S.; Brochon, C.; van de Wetering, K.; Hadziioannou, G. *Thin Solid Films* **2006**, *511−512*, 219.

(53) Zhang, Q.; Cirpan, A.; Russell, T. P.; Emrick, T. *Macromolecules* **2009**, *42*, 1079.

(54) Sommer, M.; Lang, A. S.; Thelakkat, M. *Angew. Chem., Int. Ed.* **2008**, *47*, 7901.

(55) Behl, M.; Hattemer, E.; Brehmer, M.; Zentel, R. *Macromol. Chem. Phys.* **2002**, *203*, 503.

(56) Peter, K.; Thelakkat, M. *Macromolecules* **2003**, *36*, 1779.

(57) Tew, G. N.; Pralle, M. U.; Stupp, S. I. *Angew. Chem., Int. Ed.* **2000**, *39*, 517.

(58) Sommer, M.; Lindner, S. M.; Thelakkat, M. *Adv. Funct. Mater.* **2007**, *17*, 1493.

(59) Lindner, S. M.; Thelakkat, M. *Macromolecules* **2004**, *37*, 8832.

(60) Segalman, R. A.; McCulloch, B.; Kirmayer, S.; Urban, J. J. *Macromolecules* **2009**, *42*, 9205.

(61) Botiz, I.; Darling, S. B. *Mater. Today* **2010**, *13*, 42.

(62) Darling, S. B. *Energy Environ. Sci.* **2009**, *2*, 1266.

(63) King, S.; Sommer, M.; Huettner, S.; Thelakkat, M.; Haque, S. A. *J. Mater. Chem.* **2009**, *19*, 5436.

(64) Zhang, C.; Choi, S.; Haliburton, J.; Cleveland, T.; Li, R.; Sun, S.-S.; Ledbetter, A.; Bonner, C. E. *Macromolecules* **2006**, *39*, 4317.

9265

dx.doi.org/10.1021/jp201344p |*J. Phys. Chem. C* 2011, 115, 9260–9266

(65) Lee, J. U.; Cirpan, A.; Emrick, T.; Russell, T. P.; Jo, W. H. *J. Mater. Chem.* **2009**, *19*, 1483.

(66) Herguth, P.; Jiang, X.; Liu, M. S.; Jen, A. K.-Y. *Macromolecules* **2002**, *35*, 6094.

(67) Cheng, Y.-J.; Yang, S.-H.; Hsu, C.-S. *Chem. Rev.* **2009**, *109*, 5868.

(68) Campbell, A. J.; Bradley, D. D. C.; Antoniadis, H. *Appl. Phys. Lett.* **2001**, *79*, 2133.

(69) Zhu, X.; Kahn, A. *MRS Bull.* **2010**, *35*, 443.

(70) Verduzco, R.; Botiz, I.; Pickel, D. L.; Kilbey, S. M., II; Hong, K.; Dimasi, E.; Darling, S. B. *Macromolecules* **2011**, *44*, 530.

(71) Kanai, K.; Miyazaki, T.; Suzuki, H.; Inaba, M.; Ouchi, Y.; Seki, K. *Phys. Chem. Chem. Phys.* **2009**, *12*, 273.

(72) Cook, S.; Furube, A.; Katoh, R. *Energy Environ. Sci.* **2008**, *1*, 294.

(73) Ohkita, H.; Cook, S.; Astuti, Y.; Duffy, W.; Tierney, S.; Zhang, W.; Heeney, M.; McCulloch, I.; Nelson, J.; Bradley, D. D. C.; Durrant, J. R. *J. Am. Chem. Soc.* **2008**, *130*, 3030.

(74) Korovyanko, O. J.; Österbacka, R.; Jiang, X. M.; Vardeny, Z. V. *Phys. Rev. B* **2001**, *64*, 235122.

(75) Samuel, I. D. W.; Magnani, L.; Rumbles, G.; Murray, K.; Stone, B. M.; Moratti, S. C.; Holmes, A. B. *SPIE Proc. Ser.* **1997**, *3145*, 163.

(76) Jiang, X.; Österbacka, R.; Korovyanko, O.; An, C. P.; Horovitz, B.; Janssen, R. A. J.; Vardeny, Z. V. *Adv. Funct. Mater.* **2002**, *12*, 587.

(77) Piris, J.; Dykstra, T. E.; Bakulin, A. A.; Loosdrecht, P. H. M. v.; Knulst, W.; Trinh, M. T.; Schins, J. M.; Siebbeles, L. D. A. *J. Phys. Chem. C* **2009**, *113*, 14500.

(78) Trznadel, M.; Pron, A.; Zagorska, M.; Chrzaszcz, R.; Pielichowski, J. *Macromolecules* **1998**, *31*, 5051.

(79) Guo, J.; Ohkita, H.; Benten, H.; Ito, S. *J. Am. Chem. Soc.* **2009**, *131*, 16869.

(80) Guo, J.; Ohkita, H.; Yokoya, S.; Benten, H.; Ito, S. *J. Am. Chem. Soc.* **2010**, *132*, 9631.

(81) Sun, B. Q.; Zou, G. F.; Shen, X. J.; Zhang, X. H. *Appl. Phys. Lett.* **2009**, *94*, 233504.

(82) Noone, K. M.; Anderson, N. C.; Horwitz, N. E.; Munro, A. M.; Kulkarni, A. P.; Ginger, D. S. *ACS Nano* **2009**, *3*, 1345.